Molecular cloning and subcellular distribution of the novel PDE4B4 cAMP-specific phosphodiesterase isoform

Malcolm SHEPHERD*, Theresa McSORLEY*, Aileen E. OLSEN†, Lee Ann JOHNSTON*, Neil C. THOMSON‡, George S. BAILLIE*, Miles D. HOUSLAY* and Graeme B. BOLGER†[1]

*Molecular Pharmacology Group, Division of Biochemistry and Molecular Biology, Institute of Biology and Life Sciences, University of Glasgow, Davidson Building, Glasgow G12 8QQ, Scotland, U.K., †Veterans Affairs Medical Center, Huntsman Cancer Institute, Departments of Medicine (Division of Oncology) and Oncological Science, University of Utah Health Science Center, Salt Lake City, UT 84148, U.S.A., and ‡Department of Respiratory Medicine, Western Infirmary, Glasgow, Scotland, U.K.

We have isolated cDNAs encoding PDE4B4, a new cAMP-specific phosphodiesterase (PDE4) isoform with novel properties. The amino acid sequence of PDE4B4 demonstrates that it is encoded by the *PDE4B* gene, but that it differs from the previously isolated PDE4B1, PDE4B2 and PDE4B3 isoforms by the presence of a novel N-terminal region of 17 amino acids. PDE4B4 contains both of the upstream conserved region 1 (UCR1) and UCR2 regulatory units that are characteristic of 'long' PDE4 isoforms. RNase protection demonstrated that PDE4B4 mRNA is expressed preferentially in liver, skeletal muscle and various regions of the brain, which differs from the pattern of tissue distribution of the other known PDE4B long forms, PDE4B1 and PDE4B3. Expression of PDE4B4 cDNA in COS7 cells produced a protein of 85 kDa under denaturing conditions. Subcellular fractionation of recombinant, COS7-cell expressed PDE4B4 showed that the protein was localized within the cytosol, which was confirmed by confocal microscopic analysis of living COS7 cells transfected with a green fluorescent protein–PDE4B4 chimaera. PDE4B4 exhibited a K_m for cAMP of 5.4 μM and a V_{max}, relative to that of the long PDE4B1 isoform, of 2.1. PDE4B4 was inhibited by the prototypical PDE4 inhibitor rolipram {4-[3-(cyclopentoxyl)-4-methoxyphenyl]-2-pyrrolidinone} with an IC_{50} of 83 nM. Treatment of COS7 cells with forskolin, to elevate cAMP levels, produced activation of PDE4B4, which was associated with the phosphorylation of PDE4B4 on Ser-56 within UCR1. The unique tissue distribution and intracellular targeting of PDE4B4 suggests that this isoform may have a distinct functional role in regulating cAMP levels in specific cell types.

Key words: alternative mRNA splicing, asthma, cAMP, phosphodiesterase, phosphoric ester hydrolase, rolipram.

INTRODUCTION

cAMP signalling pathways regulate numerous critical physiological processes, including those in airway smooth muscle, the immune system and the brain. A number of families of cyclic nucleotide phosphodiesterases (PDEs) hydrolyse cAMP and thus can regulate these pathways in cells. The PDE4 cAMP-specific PDEs can be differentiated from other PDE families by sequence identity in the catalytic region of the proteins and by their ability to be inhibited by a specific class of drugs, of which rolipram {4-[3-(cyclopentoxyl)-4-methoxyphenyl]-2-pyrrolidinone} is the prototype [1–3] (the nomenclature of PDE4 isoforms is outlined in [4]). Rolipram and other specific PDE4 inhibitors have antidepressant, anti-inflammatory and smooth muscle relaxant properties in humans [3]. PDE4 enzymes are also unique in having 'signature' regions of sequence, called upstream conserved regions (UCR1 and UCR2), located in the N-terminal third of the proteins [3,5].

The mammalian PDE4s are encoded by four genes (*PDE4A*, *PDE4B*, *PDE4C* and *PDE4D*), and we and other groups have shown that additional diversity in this family is produced by alternative mRNA splicing ([5–9,9a]; see [3] for a review). The use of different exons generates three groups of PDE4 isoforms: the 'long' isoforms, which contain both UCR1 and UCR2; the 'short' isoforms, which lack UCR1 but contain UCR2; and the 'super-short' isoforms, which lack UCR1 and have a truncated UCR2 [3]. In many cases, the various alternatively spliced isoforms encoded by a single gene have different patterns of expression in tissues [5–7,10–13], suggesting that they have distinct functions. In addition, the PDE4D long isoforms can be distinguished from the short isoforms by the presence of a cAMP-dependent protein kinase (PKA) phosphorylation site within UCR1, which provides a mechanism for their regulation that is unique to these long isoforms [9,9a,14–19].

We [5,8,10] and other groups [20–22] have isolated complete cDNA clones encoding three different PDE4B isoforms, and have studied their tissue distribution and biochemical properties. These isoforms differ by the substitution of unique blocks of amino acids at the N-terminal ends of their respective proteins (Figure 1A; reviewed in [3]). The human PDE4B1 isoform

Abbreviations used: BAC, bacterial artificial chromosome; EST, expressed sequence tag; GFP, enhanced green fluorescent protein; IBMX, isobutylmethylxanthine; PDE, cyclic nucleotide phosphodiesterase; PDE4, cAMP-specific phosphodiesterase; PKA, cAMP-dependent protein kinase; UCR, upstream conserved region.

[1] To whom correspondence should be addressed: University of Alabama at Birmingham, Comprehensive Cancer Center, WTI 520A, 1530 3rd Avenue South, Birmingham, AL 35294-3300, U.S.A. (e-mail Graeme.Bolger@ccc.uab.edu).

The nucleotide sequence data reported in this paper have been submitted to the GenBank®, DDBJ, EMBL and GSDB Nucleotide Sequence Databases under accession numbers AF202732 and AF202733.

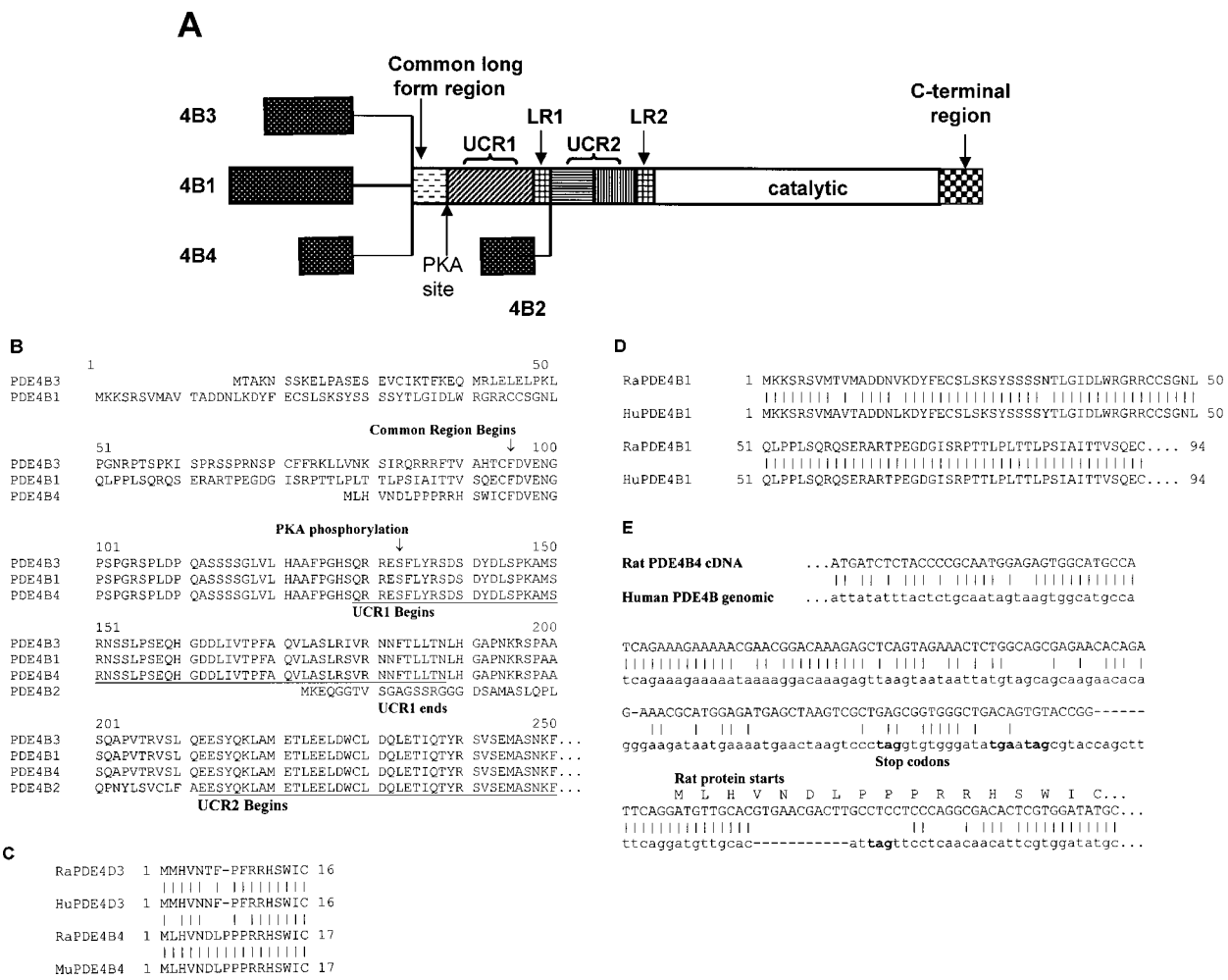

Figure 1 Structures of mRNAs and proteins encoded by the rat *PDE4B* gene

(**A**) Schematic of rat PDE4B transcripts and their encoded proteins. The four dark stippled boxes indicate the unique N-terminal regions of the proteins encoded by the following cDNAs: PDE4B1 (pRPDE89; GenBank™ AF202732); PDE4B2 (GenBank™ L27058; [10]); PDE4B3 (GenBank™ U95748; [8]); PDE4B4 (pRPDE90 and pRPDE92; GenBank™ AF202733). Also shown are regions of sequences that are highly conserved in other PDE4 isoforms, including the common long form region, UCR1 and UCR2, and the catalytic region. UCR1, UCR2 and the catalytic region are in turn separated by less conserved regions of sequence, called linker region 1 (LR1) and LR2. The C-terminal region is unique to PDE4B isoforms. The PKA phosphorylation site (PKA site) is located at the beginning of UCR1. (**B**) Alignment of the amino acid sequences of the N-terminal regions of the four rat PDE4B isoforms. Underlined regions indicate UCR1 and UCR2. Only the first 250 amino acids of the alignment are shown, as the remaining sequence is identical with that of rat PDE4B isoforms we have described previously [8,10]. An arrow indicates the PKA phosphorylation site, which is within the consensus sequence RRES. (**C**) Alignment of the amino acid sequences of the unique N-terminal regions of rat (Ra) and human (Hu) PDE4D3 and rat and mouse (Mu) PDE4B4. The PDE4D3 sequences have been published previously: GenBank™ L20970 (human; [5]) and GenBank™ U09457 (rat; [9,9a]). Vertical dashes indicate identical amino acids. Horizontal dashes indicate gaps inserted to improve the alignments. (**D**) Alignment of the amino acid sequences of the unique N-terminal regions of rat (Ra) PDE4B1 (top) and human (Hu) PDE4B1 (bottom). The sequence of human PDE4B1 has been described previously (pTM72 in [5]; GenBank™ L20966). The sequence of PDE4B4 was deduced from the pRPDE89 cDNA. (**E**) Alignment of the nucleotide sequence of the unique 5′ end of the rat PDE4B4 (pRPDE92) cDNA (capital letters) with the corresponding human genomic sequence (lower case). The human sequences correspond to nucleotides 6894–7093 of GenBank AL591487 (BAC RP11-26A10) and nucleotides 67803–67604 of GenBank AL356437 (BAC RP4-639A9), which are identical in this region. The vertical dashes indicate identity between the two sequences; horizontal dashes indicate gaps inserted by the program to improve the alignments. The amino acid sequence of rat PDE4B4 is shown above its corresponding cDNA sequence. Also shown are the stop codons located in the human sequence.

encodes a protein of 736 amino acids [5]. A second isoform, PDE4B2, encodes a protein of 564 amino acids in humans [5,20,21] and rats [10,22]. A third isoform, PDE4B3, encodes a protein of 721 amino acids [8]. Both the PDE4B2 and PDE4B3 isoforms are strongly conserved among species, with the human and rat counterparts being of identical length and sharing over 90% amino acid sequence identity [8,10].

There would be considerable value in determining the full range of PDE4 isoforms that are present in mammals. This information is essential for genetic and physiological studies of these genes. For example, identification of the complete family of isoforms encoded by the *PDE4B* gene will be necessary in order to determine their individual contributions to the phenotype of mice with targeted mutations of the *PDE4B* gene [23]. It may also be of pharmacological value, as there is currently considerable interest in developing PDE4 inhibitors as therapeutic agents, particularly for lung diseases such as asthma [24–29]. Pharmacological studies have suggested that the cell types responsible for the therapeutic effects of these drugs may have a pattern of PDE4 expression that differs from that in cells responsible for their undesirable side effects [25–27,29], and that the isoforms present in different tissues may have distinct sensitivities to particular PDE4 inhibitors. Identification of the full range of PDE4 isoforms, and determination of their

differential expression in tissues, will be essential for understanding the molecular basis of these pharmacological effects.

We now describe the cloning of a cDNA, pRPDE90, which encodes a fourth PDE4B isoform, which we call PDE4B4. pRPDE90 was isolated from rat brain, and encodes a protein of 659 amino acids that is present in a wide spectrum of tissues, including the brain. PDE4B4 differs from other long PDE4B isoforms in that it contains a unique N-terminal region of 17 amino acids. Unlike other the long PDE4 isoforms that we have studied [7,8,30–32], PDE4B4 is found exclusively in the cytosol of transfected COS7 cells. It is also more active than the long PDE4B1 isoform, indicating that its unique N-terminal region can regulate its catalytic activity. Finally, we show that PDE4B4 is phosphorylated and activated by the action of PKA.

EXPERIMENTAL

Isolation and analysis of cDNA clones

Procedures were as described by Sambrook and Russell [33], unless specified otherwise. A rat (*Rattus norwegenesis*; Sprague–Dawley strain) cerebral cortex cDNA library, cloned into the *Eco*RI site of Lambda ZAPII, was obtained from Stratagene. The cDNA library was screened by hybridization with a probe corresponding to nucleotides 204–1299 of rat PDE4B3 (GenBank™ accession number U95748 [8]). Hybridization was performed with a final wash in $0.3 \times$ SSC/0.3 % SDS at 62 °C ($1 \times$ SSC is 0.15 M NaCl, 0.015 M sodium citrate). Sequencing was performed on both strands with an ABI Prism sequencer (Perkin-Elmer) according to the manufacturer's instructions. Alignments were generated with the Gap and Lineup programs of the Wisconsin Package of UNIX sequence software programs (Oxford Molecular Group), using the standard defaults.

RNase protection analysis

This was performed exactly as we have described previously for other PDE4 isoforms [5–7,10]. The probe designed to detect all rat PDE4B isoforms corresponds to the 3′ untranslated region of the pDPD mRNA (nucleotides 1896–2112, GenBank™ accession number J04563; [10,34]). The probes specific for PDE4B3 and PDE4B4 correspond to the unique 5′ ends of their mRNAs, specifically nucleotides 204–668 of rat PDE4B3 and nucleotides 1–312 of pRPDE92 (PDE4B4).

Generation and expression of PDE4B mammalian cell expression constructs

The full open reading frame of each of rat PDE4B2 (GenBank™ accession number L27058 [10]), PDE4B3, pRPDE89 and pRPDE90 were cloned into the *Not*I site of pcDNA3 (Invitrogen), placing them under the control of the cytomegalovirus intermediate early gene promoter. These constructs were prepared by the addition of *Not*I sites to the cDNAs by the use of PCR, as described previously [5]. A Kozak consensus site [35] was also added just upstream of the start codon. A sequence corresponding to the FLAG epitope [36] was added immediately downstream from the last codon of the PDE to encode a C-terminal fusion. The native PDE4B stop codon was removed in this process, but a synthetic stop codon was placed immediately downstream from the epitope sequence. For expression of enhanced green fluorescent protein (GFP) fusion proteins in mammalian cells, the full pRPDE90 open reading frame was cloned into the *Not*I site of pEGFP-C1 (Clontech) to produce a fusion between the C-terminal end of *Aequorea victoria* GFP and the N-terminus of PDE4B4.

Site-directed mutagenesis

The circular mutagenesis technique [33] was used to mutate codon 56 of PDE4B4 from serine to alanine. All PCR-generated or mutagenized constructs were verified by sequencing prior to use.

Expression of cDNAs in COS7 cells

COS7 simian virus 40-transformed monkey kidney cells were grown at 37 °C in 5 % CO_2 in Dulbecco's modified Eagle's medium supplemented with 10 % (v/v) fetal bovine serum, 2 mM glutamine and antibiotics. The cells were transfected as described previously [6,8,31]. In brief, the cells were grown to 70 % confluence and the medium was changed to Dulbecco's modified Eagle's medium plus 0.1 mM chloroquine. A 5 μg portion of plasmid DNA, mixed with 250 μl of 10 mg/ml DEAE-dextran in PBS, was added to the cells, and they were incubated for 4 h at 37 °C. The medium was removed and the cells were treated with 10 % (v/v) DMSO in PBS, washed once with PBS, and incubated for 48 h. In some cases (see the Results section), the transfected COS7 cells were plated into six-well plates and grown without serum overnight before being treated with various drugs.

Preparation of subcellular fractions from COS7 cells

This was performed as described previously [6,8,31,32]. In brief, transfected COS7 cells were grown as above. The medium was aspirated and the cells were washed twice with ice-cold PBS, followed by a wash with ice-cold KHEM buffer [50 mM KCl, 10 mM EGTA, 1.92 mM $MgCl_2$, 1 mM dithiothreitol, 50 mM Hepes, pH 7.2, containing Complete™ protease inhibitor cocktail (Roche Molecular Systems)], and then snap-frozen in liquid nitrogen. The frozen cells were thawed on ice and lysed by passing them 10 times through a 26.5-gauge needle. They were then centrifuged at 1000 ***g*** for 10 min to produce a low-speed pellet (P1 fraction) and a low-speed supernatant (S1). S1 was then centrifuged at 100 000 ***g*** for 60 min to produce a high-speed pellet (P2 fraction). The pellet fractions were resuspended in KHEM buffer.

Generation and characterization of antibodies

All procedures for the generation and use of PDE4B-specific antibodies were as described previously by us [8]. The M2 monoclonal antibody to the FLAG epitope [36] was obtained from Roche Molecular Systems. A polyclonal antibody (PS54-UCR1-A1) that detects the phosphoserine form of the PKA phosphorylation site, located in the UCR1 of all PDE4 long isoforms, was used as described by us previously [37]. In brief, the phosphopeptide of sequence SQ**RRES***FLYRSDSDYDLSP was used as antigen, and also to block the interaction of the PS54-UCR1-A1 antibody with its epitope (the phosphoserine in the peptide is indicated by *, and the PKA consensus phosphorylation site is indicated by bold type).

Immunopurification

Selective immunopurification of FLAG-tagged recombinant PDE4B4 was performed with anti-FLAG M2–agarose beads (Sigma) using procedures described by us previously in detail [37,38]. In all cases, it was ensured that sufficient anti-FLAG antibody was present to immunoprecipitate all of the recombinant PDE4B4 in the sample, usually 50 μl of beads per 90 μg of protein from clarified cell lysates, in a total volume of 200 μl of KHEM buffer [37,38].

SDS/PAGE and immunoblotting

These were performed as described previously [7,8,30–32]. In brief, samples (2–50 μg of protein/lane) were resuspended in Laemmli buffer [39] and boiled for 5 min. Gels containing 8 % (w/v) acrylamide were run at 8 mA overnight or at 50 mA for 4–5 h with cooling. Nitrocellulose membranes were blocked in 5 % (w/v) low-fat milk powder in TBS (10 mM Tris/HCl, pH 7.4, 150 mM NaCl) overnight at room temperature. They were then incubated with various antibodies (described above) diluted 1:2000 (v/v) in 1 % (w/v) low fat milk powder in TTBS (TBS plus 0.1 % Tween 20) for 3 h at room temperature. Detection of the bound antibody was performed with donkey anti-(rabbit IgG)–peroxidase antibody and the enhanced chemiluminescence system (ECL®; Amersham).

PDE assays

PDE activity was assayed as described previously [40]. All assays were performed at 30 °C, and a freshly prepared slurry of Dowex/water/ethanol (1:1:1, by vol.) was used in all experiments. Initial rates were taken from linear time courses of activity. K_m values were determined over a substrate range of 0.25–25 μM cAMP (10 different concentrations). Dose-dependent inhibition by rolipram was determined in the presence of 1 μM cAMP and over the range 0.1 nM–10 μM inhibitor. The IC_{50} was then determined from these values, using a least-squares fitting algorithm. Rolipram was dissolved in 100 % DMSO as a 1 mM stock and diluted in 20 mM Tris/HCl, pH 7.4, and 10 mM $MgCl_2$ to provide the range of concentrations used in the assay. The residual amounts of DMSO were shown not to affect PDE activity at the levels used in this study. To define K_m values, data from PDE assays were analysed by computer fitting to the hyperbolic form of the Michaelis–Menten equation using an iterative least-squares procedure (Ultrafit; with Marquardt algorithm, robust fit, experimental errors supplied; Biosoft). V_{max} values were calculated using the Michaelis–Menten equation and the experimentally derived K_m values, as described previously [32]. As described by us previously [8,31], relative V_{max} values were obtained by using equal amounts of immunoreactive PDE4B protein, as determined with PDE4B-specific antibodies in both ELISA and quantitative immunoblotting. Total PDE activity was determined at a substrate concentration of 1 μM cAMP, and was defined as the amount of PDE activity that could be inhibited by 10 μM rolipram. At this concentration, rolipram is a PDE4-selective inhibitor, and can completely inhibit PDE4 activity [3]. As we have described previously [17,37], in transfected COS7 cells more than 98 % of total PDE activity was due to the recombinant PDE4 enzyme.

Measurement of protein concentration

Protein concentrations were measured by the method of Bradford [41], using BSA as a standard.

Confocal microscopy

This was performed as we have described previously [30]. Briefly, COS7 cells were seeded at 40 % confluency on to 22 mm-diameter coverslips 24 h prior to transfection. They were transfected with 2 μg of plasmid DNA using DOTAP {*N*-[1-(2,3-dioleoyloxy) propyl]-*N*,*N*,*N*-trimethylammonium methylsulphate; Roche Molecular Systems} for 16 h. They were then washed, incubated in medium for a further 32 h, and then examined at room temperature with a Zeiss laser scanning confocal microscope consisting of an Axiovert 100 microscope with a $\times$63/1.4 NA plan apochromat objective. Image analysis was carried out using the Improvision Open Lab System (Carl Zeiss).

RESULTS

Isolation of rat cDNAs encoding novel PDE4B isoforms

To search for cDNAs encoding novel PDE4 isoforms, we screened a rat brain cortex cDNA library with a probe corresponding to the unique N-terminal region, UCR1 and the majority of UCR2 of rat PDE4B3 [8]. This probe was designed to detect all long PDE4B isoforms (Figure 1A). cDNAs encoding

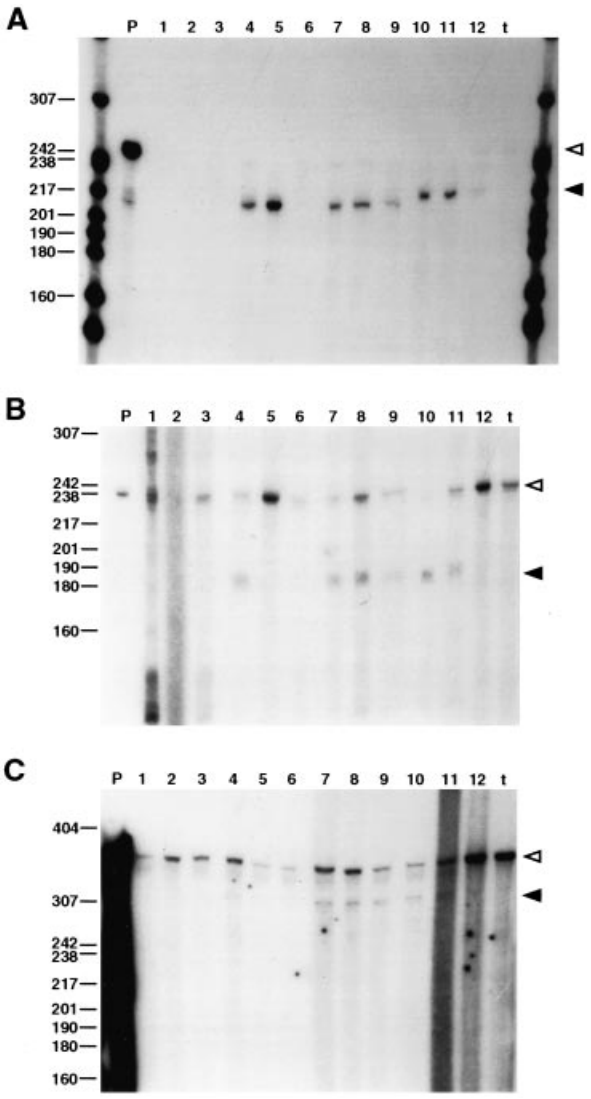

Figure 2 Tissue distribution of rat PDE4B mRNAs, as determined by RNase protection

Total RNA (10 μg) was isolated from various rat tissues and analysed by RNase protection [33] with the following probes: (**A**) a probe corresponding to the 3′ sequence of all known PDE4B RNAs, as described previously [10]; (**B**) a probe corresponding to the 5′ end of PDE4B3; (**C**) a probe corresponding to the 5′ end of PDE4B4. The short horizontal lines on the sides of the panels indicate size markers (in nucleotides). Open arrowheads indicate the migration of the intact probe, and filled arrowheads indicate the migration of the protected fragment. Lanes are as follows: P, probe without RNase; 1, kidney; 2, testis; 3, heart; 4, lung; 5, spleen; 6, liver; 7, brainstem; 8, cerebellum; 9, occipital cortex; 10, parietal cortex; 11, temporal cortex; 12, frontal cortex; t, tRNA (10 μg).

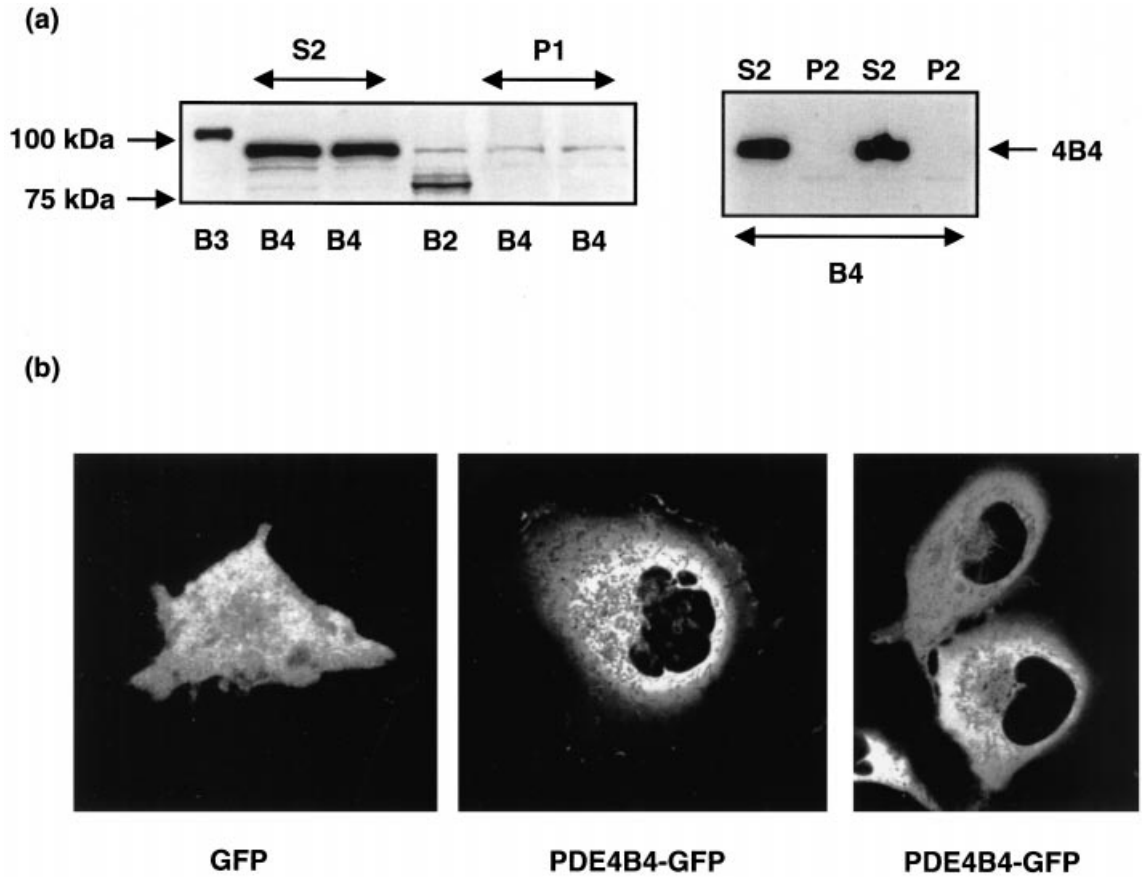

Figure 3 Subcellular distribution of PDE4B4 in transfected COS7 cells

(**a**) COS7 cells were transfected with plasmids encoding the indicated PDE4B isoform, and then harvested and fractionated to produce low-speed (P1), high-speed (P2) and high-speed supernatant (S2) fractions (see the Experimental section). The fractions were analysed by SDS/PAGE and immunoblotted with a PDE4B-specific antibody. The PDE4B2, PDE4B3 and PDE4B4 isoforms migrate at 78 kDa, 103 kDa and 85 kDa respectively. (**b**) Single optical sections through the centre of transfected COS7 cells, obtained by laser scanning confocal microscopy. The cells were transfected with plasmids encoding GFP or the PDE4B4–GFP chimaera, as indicated. The data are typical of experiments done on three different transfections.

two different PDE4B isoforms were detected in the screen. One of these clones encoded the PDE4B1 isoform, as described in detail below. The other cDNA clone, called pRPDE90, encoded the complete open reading frame of a novel PDE4B isoform. We called this new isoform PDE4B4, using the accepted nomenclature [4]. The PDE4B4 protein consists of 659 amino acids, 16 of which are located at the extreme N-terminal end of the protein and show no detectable identity with any previously cloned PDE4B sequence (Figure 1B). The remaining 643 amino acids are identical with the corresponding regions of the long PDE4B isoforms PDE4B1 and PDE4B3 (Figure 1B). The nucleotide sequences of the common regions of PDE4B1, PDE4B3 and PDE4B4 are also identical. The sequence of the novel region of PDE4B4 was confirmed by the sequence of another clone isolated in the screen, called pRPDE92, which completely overlapped the novel region of pRPDE90 and contained sequence of an additional portion of the 5′ untranslated region of the mRNA. In addition, there was strong amino acid sequence similarity between the unique N-terminal end of PDE4B4 and the corresponding unique N-terminal ends of the human and rat PDE4D3 sequences (Figure 1C), which provides additional evidence for the fidelity of the pRPDE90 and pRPDE92 cDNAs.

Also detected in the screen was a cDNA clone, pRPDE89, which encoded a novel protein of 736 amino acids (Figures 1B and 1D). This protein was identical in length and had greater than 96% amino acid identity (712 out of 736 amino acids) with the human PDE4B1 isoform [5]. This similarity included the unique N-terminal regions of the two proteins (90 out of 96 amino acids identical; Figure 1D) [5]. We therefore concluded that pRPDE89 encodes the rat PDE4B1 isoform.

Analysis of mouse DNA sequences corresponding to rat PDE4B4

In silico analysis of mouse DNA sequences in publicly available databases did not detect any cDNAs or ESTs (expressed sequence tags) that corresponded to the unique 5′ end of PDE4B4. However, this analysis identified a mouse genomic sequence within the bacterial artificial chromosome (BAC) clone RP23-192K24, located on chromosome 4, that was 95% identical at the nucleotide level with that of the unique region of pRPDE92. This mouse DNA sequence contained an open reading frame that encoded a protein sequence identical with the unique region of the rat PDE4B4 protein (Figure 1C). Although we have not cloned the corresponding mouse cDNA, the strong identity between these sequences suggests that an exon corresponding to that of rat PDE4B4 exists in mice. Further analysis of the RP23-192K24 clone demonstrated that it clearly contained discrete,

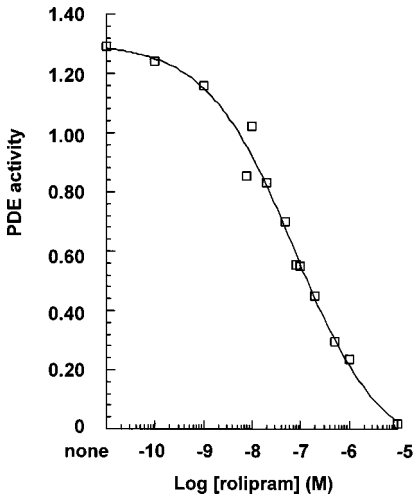

Figure 4 Inhibition of PDE4B4 by rolipram

A dose–response curve for the inhibition of PDE4B4 enzymic activity by rolipram was obtained, using COS7 cell extracts assayed with 1 μM cAMP as substrate. This plot is typical of data obtained with three different transfections.

widely separated blocks of sequence with high identity with the unique 5′ ends of the PDE4B1 and PDE4B3 mRNAs, consistent with the concept that the respective 5′ ends of the PDE4B1, PDE4B3 and PDE4B4 mRNAs are each derived from separate exons.

Analysis of human DNA sequences corresponding to rat PDE4B4

We also performed an *in silico* analysis of human DNA sequences available in publicly available databases. No human cDNAs or ESTs that corresponded to the unique 5′ end of the pRPDE92 cDNA were detected. However, human genomic sequence that was very similar to the unique 5′ end of the pRPDE92 cDNA was identified independently in two different BAC clones, RP11-26A10 and RP4-639A9 (Figure 1E). The RP11-26A10 BAC has also been shown to overlap two other BAC clones (RP11-360-E7 and RP4-543C6). We detected several previously known PDE4B exons in RP11-360-E7 and RP4-543C6, although these BACs have not been sequenced completely and a fully assembled contig is not available at this time. Additionally, all four BACs have been mapped by the Sanger Center (Cambridge University, Cambridge, U.K.) to chromosome 1p31–32, which we have shown previously to be the location of the human *PDE4B* gene [42]. Therefore we concluded that the sequences on the RP11-26A10 and RP4-639A9 BACs are located within the human *PDE4B* gene and correspond to the rat PDE4B4 exon.

Comparison of the human and rat PDE4B4 exons demonstrated substantial differences between their predicted protein-coding sequences (Figure 1E). The human DNA sequence is missing regions of sequence within a region that is otherwise highly similar to sequence that encodes the rat PDE4B4 protein. In addition, the human sequence has tightly clustered stop codons in all three possible reading frames just upstream from the region with identity to the rat-protein-coding sequence, and only two start codons (ATG) in any reading frame downstream from the stop codons. Translation initiating at either of these start codons would not generate a biochemically active PDE4 protein. Therefore we conclude that the human PDE4B4 exon is unlikely to encode a protein. Indeed, it may not be transcribed (i.e. it could be a 'dead' exon).

Tissue expression of PDE4B mRNAs

The tissue distributions of rat PDE4B mRNAs were determined by RNase protection. To detect transcripts specific to PDE4B3 and PDE4B4, we used probes corresponding to the unique 5′ ends of the PDE4B3 and PDE4B4 mRNAs (Figures 2B and 2C). The PDE4B3 mRNA appeared to be expressed throughout the brain, and also in heart, lung and liver, while the PDE4B4 mRNA was detected only in liver and brain. As a comparison, a single-stranded antisense RNA probe corresponding to the 3′ end of the PDE4B1 isoform, which would detect all known PDE4B isoforms (Figure 1A), was used to probe total RNA isolated from various rat tissues (Figure 2A). Using this probe, transcripts from the *PDE4B* gene were detected in a wide variety of rat tissues, consistent with results that we and others have described previously [10,22,34]. We have also reported previously the tissue distribution of PDE4B1 mRNA [10].

Expression of PDE4B cDNAs in COS7 cells

We wished to determine the biochemical properties of the PDE4B4 isoform, so that they could be compared with those of the three other PDE4B isoforms that we have characterized previously [8]. As the vast majority of tissues that have been examined to date contain multiple PDE4 isoforms [43], it is difficult to determine the enzymic properties of any individual isoform in extracts from these cells. Therefore we have developed a system in which cDNAs encoding the various isoforms are transiently expressed in COS7 cells. This allows the properties of individual recombinant PDE4 isoforms to be compared directly in the same cell background [6,7,31]. For this purpose, PDE4B isoforms were transiently expressed in COS7 cells from cDNAs expressed under the control of the cytomegalovirus intermediate early gene promoter.

Extracts from COS7 cells transfected with a plasmid encoding PDE4B4 were fractionated to yield low-speed (P1) and high-speed (P2) pellet fractions, along with a high-speed supernatant (S2) or cytosolic fraction, as described in the Experimental section. These fractions were then analysed by SDS/PAGE and immunoblotted with a PDE4B-specific antibody (Figure 3a). The novel PDE4B4 isoform migrated as a single immunoreactive band of 84 ± 4.5 kDa ($n = 4$ separate transfections). PDE4B4 thus migrates distinctly from the other PDE4B isoforms, namely PDE4B1 (104 kDa), PDE4B2 (78 kDa) and PDE4B3 (103 kDa; [8]). To confirm these data, a single immunoreactive band of 86.5 ± 3.0 kDa was seen in PDE4B4-transfected COS7 cells upon immunoblotting with the anti-FLAG antibody, which detected the C-terminal FLAG tag incorporated into the PDE4B4 expression construct. In contrast, no immunoreactive material was identified in non-transfected or mock-transfected COS7 cells.

We have reported previously that the PDE4B1 and PDE4B3 isoforms have a molecular mass as determined by their mobility in SDS/PAGE of approx. 20 kDa greater than that predicted from their amino acid sequence [8]. This is also the case for PDE4B4, which migrates at 86 kDa in SDS/PAGE (Figure 3a), while its predicted size on the basis of its amino acid sequence would be 73 kDa. It is possible that this may reflect particular conformational properties, or anomalous binding to SDS, of these proteins in SDS/PAGE. Similar anomalous migration in SDS/PAGE has been observed previously for recombinant and native PDE4A [7,31] and PDE4D [6] isoforms.

When we analysed the subcellular distribution of COS7-expressed recombinant PDE4B4, we found that PDE4B4 was

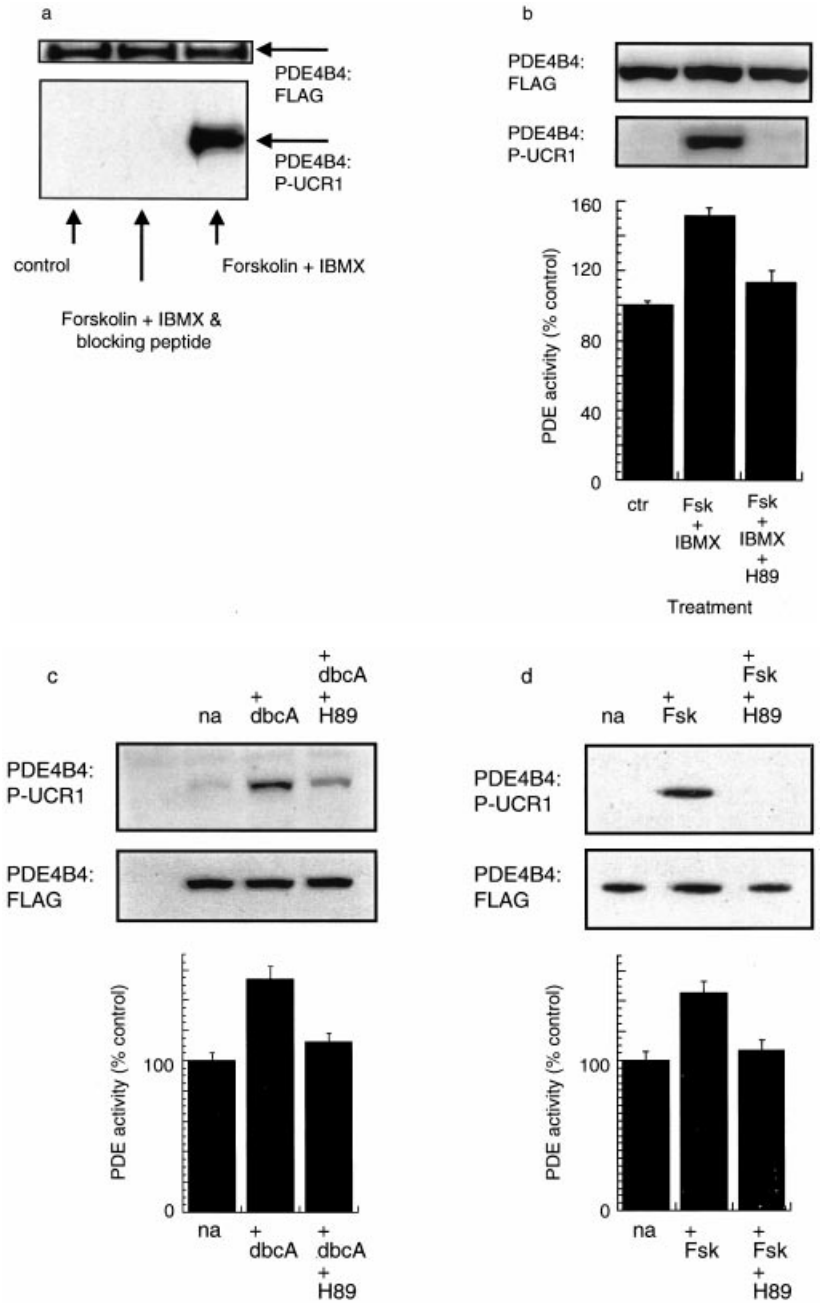

Figure 5 Activation of PDE4B4 by PKA

(**a**) Immunoblots with the anti-FLAG antibody (upper) or the PS54-UCR1-A1 antibody (lower) of extracts of COS7 cells transfected to express FLAG-tagged PDE4B4. Extracts from cells treated with 100 μM forskolin plus 100 μM IBMX for 15 min are shown, along with untreated controls. Also shown is a parallel lane in which a 10-fold excess of the peptide used to make the antibody was added during immunoblotting, as a control for its specificity. The data are typical of three separate transfections. (**b**) COS7 cells were transfected with PDE4B4, subjected to various treatments, and then disrupted for measurement of PDE4 activity. In the bottom panel, PDE4 activity is expressed as a percentage of that present in untreated cells (ctr). Fsk, 100 μM forskolin; IBMX, 100 μM IBMX; H89, 0.5 μM H89. The data are shown as means $\pm$ S.D. of three different transfections. In the upper panels are immunoblots for these three conditions from typical experiments, using the anti-FLAG antibody to assess loading (top), and the PS54-UCR1-A1 antibody to assess phosphorylation (middle). (**c**) As for (**b**), but the cells were treated or not (na) for 10 min with 100 μM dibutyryl cAMP (dbcA) with or without H89. (**d**) COS7 cells were transfected with FLAG-tagged PDE4B4 and then treated with a combination of forskolin and IBMX for 15 min, with or without H89. They were then disrupted and PDE4B4 was immunopurified with anti-FLAG–agarose beads. PDE4 activity was then measured in the immunopurified material. In the upper panels are immunoblots for these three conditions from typical experiments, using the PS54-UCR1-A1 antibody to assess phosphorylation (top), or the anti-FLAG antibody to assess loading (middle). Each immunoblot is typical of experiments performed three times. PDE4 activity is expressed as mean $\pm$ S.D. of three different transfections.

present only in the S2 fraction (Figure 3a), while the three other PDE4B isoforms, when expressed in COS7 cells, partitioned between both the S2 and P2 fractions [8]. To obtain independent confirmation of the cytosolic location of PDE4B4, we prepared a chimaera between PDE4B4 and GFP, and expressed it in COS7 cells. The localization of the chimaera in living cells was determined by confocal microscopy. COS7 cells transfected with GFP alone showed fluorescence that was distributed throughout

the cell, including the nucleus (Figure 3b). However, COS7 cells transfected with the PDE4B4–GFP chimaera showed fluorescence throughout the cell cytosol, with clear evidence of nuclear exclusion (Figure 3b). The fluorescence also appeared to be excluded from various vesicular structures in the transfected COS7 cells, such as the Golgi apparatus and plasma membrane. These data are consistent with the immunoblotting data showing that PDE4B4 partitions predominantly in the S2 fraction. As disruption of cells for biochemical analyses may release weakly associating membrane proteins, it is therefore reassuring to confirm the essentially cytosolic distribution of the PDE4B4–GFP chimaera in living cells.

Enzymic properties of the novel recombinant PDE4B4 isoform

Lysates from mock-transfected (vector only) COS7 cells had a cAMP PDE activity of 9 ± 3 pmol/min per mg of protein, which was not different from that in untransfected COS7 cells (8 ± 3 pmol/min per mg). In contrast, lysates of COS7 cells transfected with constructs expressing PBE4B4 had a cAMP PDE activity of 529 ± 43 pmol/min per mg (means $\pm$ S.D.; $n = 3$ separate transfections). Greater than 98 % of this activity was inhibited by the PDE4-selective inhibitor rolipram (10 μM; at a concentration of 1 μM cAMP). At least 95 % of the PDE4 activity was found in the S2 fraction ($n = 5$), consistent with the immunoblotting and confocal microscopy data indicating that PDE4B4 is located within the cytosol in transfected COS7 cells.

Analysis of PDE4B4 activity from the S2 fraction showed it to have a K_m for cAMP of 5.4 ± 1.0 μM ($n = 4$ separate transfections). We also wished to determine the V_{max} of PDE4B4, relative to that of other PDE4B isoforms. As we have shown previously for other PDE4 isoforms [6–8], it is possible to obtain a relative V_{max} by normalizing for the amount of PDE4 protein in cell extracts, as measured by immunoblotting. This is possible because the various active proteins encoded by a single gene have identical catalytic regions and C-termini, and therefore can be measured by immunoblotting with antibodies to the C-terminal region of the proteins. Therefore we compared the V_{max} of PDE4B4 with that of PDE4B1. If the V_{max} of PDE4B1 is set at 1.0, then the relative V_{max} of PDE4B4 was determined to be 2.1 ± 0.2 ($n = 4$ separate transfections). We have shown previously that the cytosolic forms of PDE4B2 and PDE4B3 have relative V_{max} values of 3.8 and 1.6 respectively compared with that of cytosolic PDE4B1. Thus the V_{max} values of the two long PDE4B isoforms, i.e. PDE4B3 and PDE4B4, appear to be similar. These relative V_{max} values assume either that the recombinant PDE4B isoforms are expressed in COS7 cells as fully functional proteins or, if as proteins with crippled activities, that the crippling of activity occurs to a similar extent for all the PDE4B isoforms. Given that these PDE4B isoforms have identical catalytic and C-terminal regions, it is most likely that recombinant active enzymes will be generated similarly in each instance.

The PDE4-selective inhibitor rolipram inhibited PDE4B4 activity with an IC_{50} of 83 ± 24 nM ($n = 4$ separate transfections) (Figure 4). This compares with IC_{50} values of 80, 20 and 50 nM for PDE4B1, PDE4B2 and PDE4B3 respectively, as determined previously [8]. Therefore the cytosolic forms of all PDE4B isoforms appear to be inhibited similarly by rolipram.

Activation of PDE4B4 by PKA

The long PDE4D3 isoform has been shown to be activated by the phosphorylation of Ser-54 [9,9a,14–19,44]. This target serine is located within a well-defined PKA consensus phosphorylation motif, of sequence Arg-Arg-Glu-Ser, that is located at the beginning of UCR1 and which is conserved in all long PDE4 isoforms. The corresponding serine in PDE4B4 is Ser-56 (Figure 1B). We have developed an antibody, PS54-UCR1-A1, that recognizes this specific phosphoserine in all PDE4 isoforms ([37,44]; see also the Experimental section). Using this antibody, we found no immunoreactive material in untreated COS7 cells expressing PDE4B4 (Figure 5a). However, when these cells were treated for 15 min with the adenylate cyclase activator forskolin (100 μM) and the non-selective PDE inhibitor isobutylmethylxanthine (IBMX; 100 μM), which together raise intracellular cAMP levels [45], we identified a single 85 kDa immunoreactive band consistent with phosphorylated PDE4B4 (Figure 5a). This signal was eliminated by preincubation of the antibody with the peptide used originally to generate the antibody. These data indicate that elevation of intracellular cAMP levels in COS7 cells results in phosphorylation of PDE4B4 by PKA.

We next determined whether phosphorylation of PDE4B4 affected its enzymic activity. COS7 cells were transfected with PDE4B4 and then treated with forskolin and IBMX. Extracts from these cells were then assayed for PDE4 activity. Treatment with forskolin and IBMX together produced an approx. 50 % increase in activity (Figure 5b), which could be blocked by the PKA inhibitor H89 (0.5 μM). We estimate that any carry-over of IBMX from the cells into the PDE assays had no effect on PDE4B4 enzymic activity, as it would be diluted to less than 1 nM in the assay. These treatments consistently increased the phosphorylation of PDE4B4 at Ser-56, as demonstrated by immunoblotting with the PS54-UCR1-A1 antibody (Figure 5b). Treatment of PDE4B4-transfected COS7 cells with the cell-permeant cAMP analogue dibutyryl cAMP (100 μM) both produced an activation of PDE4B4 similar to that seen with combined forskolin and IBMX treatment and resulted in Ser-56 phosphorylation, as demonstrated by PS54-UCR1-A1 immunoblotting (Figure 5c). Both of these effects were ablated by the PKA inhibitor H89 (1 μM; Figure 5c).

Additionally, we immunopurified recombinant FLAG-tagged PDE4B4 from transfected COS7 cells using an anti-FLAG antibody (Figure 5d). This FLAG-tagged PDE4B4 was activated similarly in COS7 cells after combined forskolin and IBMX treatment. This activation was ablated by H89 and was associated with PDE4B4 phosphorylation, as demonstrated by PS54-UCR1-A1 immunoblotting (Figure 5d). The PDE4B4 immunopurified from cells after combined forskolin and IBMX treatment had a K_m for cAMP of 4.9 ± 0.7 μM ($n = 3$), similar to that of PDE4B4 isolated from untreated cells (5.1 ± 0.8 μM; $n = 3$).

We conclude that the PKA-mediated phosphorylation of Ser-56 in UCR1 of PDE4B4 leads to activation of this long isoform. Consistent with this, we failed to observe any increase (< 5 % change) in the activity of a Ser-56 $\rightarrow$ Ala mutant expressed in COS7 cells after treatment with a combination of forskolin and IBMX or with dibutyryl cAMP.

DISCUSSION

We describe here a novel PDE4B isoform that is expressed in multiple rat tissues, including the brain and lung. This novel isoform, which we call PDE4B4, has an N-terminal region of 17 amino acids that is not present in any other PDE4B isoform. In addition, it contains both the UCR1 and UCR2 regulatory regions, defining it as a long PDE4 isoform. It is highly likely that the PDE4B4 mRNA, like those of PDE4B1 and PDE4B3, is generated by alternative mRNA splicing and the use of separate transcriptional start sites. A similar pattern of alternative mRNA

splicing generates the PDE4A and PDE4D isoforms ([6,7]; see [3] for a review). The point of divergence between PDE4B1, PDE4B3 and PDE4B4 corresponds to the major point of alternative mRNA splicing in transcripts from the *PDE4A* [5], *PDE4B* [8] and *PDE4D* [6,9,9a] genes and from the homologous *dunce* gene of *Drosophila melanogaster* [46]. It also corresponds to the 5′ end of an exon in the human *PDE4A* [47] and the mouse *Pde4a* [48] genes. Furthermore, as there is no region of sequence common to the 5′ ends of any of these cDNAs, it is likely that each is generated from a different transcriptional start site.

Although PDE4B4 is expressed in multiple rat tissues and is also likely to be present in the mouse, it does not appear to be present in humans. This result was unexpected, as almost all of the PDE4 isoforms that we have identified to date have corresponding homologues in humans and rodents [3]. In view of the conservation of the PDE4B4 sequence among rodents (mouse and rat), it is likely that PDE4B4 has an essential function in rodents. Since PDE4B4 is not present in humans, it is possible that this essential function is not required in humans or that other PDE4 isoforms, such as PDE4D3, have taken over this function in humans. This finding has implications for the extrapolation of data obtained with rodent models to humans. For example, the mouse PDE4B knockouts that have been reported to date have disruptions in exons encoding the PDE4B catalytic region, which eliminates the expression of all PDE4B isoforms in these mice [23]. The precise function of PDE4B4 could be determined by knocking out only the PDE4B4-specific exon. Since the precise contribution of PDE4B4 to the phenotype of these mice has not been determined, some caution may be appropriate in extrapolating results obtained with these mice to humans (i.e. beyond that normally encountered in comparing the two species).

PDE4B4 differs from all other PDE4 isoforms characterized previously (see [2,3] for reviews) in that it has minimal, or no, association with cellular particulate fractions when expressed in COS7 cells. The only other known PDE4 isoforms that are essentially cytosolic when expressed in COS7 cells are the short isoforms, PDE4D1 and PDE4D2 [6]. The unique N-terminal regions of each of the various PDE4 isoforms are critical in determining their targeting to membranes, and this targeting is compatible with the interaction of the various PDE4 isoforms with different membrane anchoring proteins [2,3]. However, we do not know the full range of anchor proteins for the PDE4s or the full pattern of expression of the anchor proteins in cells or tissues. Therefore we cannot be certain whether the lack of membrane association of PDE4B4 in COS7 cells reflects an inherent inability of PDE4B4 to associate with membranes, or is because an appropriate anchor protein is not expressed in COS7 cells, or is because some modification of PDE4B4 or its anchor is necessary for membrane association. In this regard, we and others have shown that one other long PDE4 isoform, PDE4D3, associates with different 'anchor' proteins in different cell types [49–51]. Alternatively, it may be that PDE4B4 interacts with a soluble signalling scaffold protein, as has been shown for PDE4D5 and RACK1 (receptor for activated c-kinase), which can be isolated in a cytosolic complex [52].

PDE4B isoforms do not appear to differ greatly with regard to V_{max} for cAMP hydrolysis. In the present study, we showed that the maximal activity of PDE4B4 is double that of another long isoform, PDE4B1, and similar to that of the PDE4B3 isoform. The K_m for cAMP of PDE4B4, 5 μM, is about double that of other PDE4B isoforms [8]. In contrast, the cytosolic forms of all long PDE4B isoforms are similarly sensitive to inhibition by rolipram, with IC_{50} values in the range 50–80 nM, although the short PDE4B2 isoform is more sensitive (20 nM; [8]). The physiological significance of these differences remains to be determined. Nonetheless, given that small changes in adenylate cyclase activity can lead to profound differences in cAMP accumulation and cell function, then the converse is likely to be true for PDEs.

Several groups, including ours, have shown that the long PDE4D3 isoform can be activated by PKA-mediated phosphorylation at Ser-54 within UCR1 [9,9a,14–19]. This serine is conserved in all PDE4 long isoforms, including those of PDE4B [3]. In the present study, we use a novel phospho-specific antiserum [37,44] to show that elevation of cAMP levels in COS7 cells can result in phosphorylation of the corresponding serine in PDE4B4 (Ser-56). This phosphorylation is also associated with activation of PDE4B4 in a PKA-dependent fashion. It has been suggested that a physiological role for the activation of PKA phosphorylation by phosphorylation may be to contribute to cellular desensitization of cAMP signalling [1], and it is possible that phosphorylation of PDE4B4 serves a similar role in the cells where it is expressed.

The unique N-terminal region of PDE4B4 is likely to confer specific properties on this isoform, by analogy with other PDE4 isoforms [2,3]. These differences are likely to include its intracellular targeting, as well as its differences in V_{max} and K_m for cAMP relative to other PDE4B isoforms. These differences provide potential mechanisms for understanding the functional significance of PDE4B4 in cells and tissues.

G. B. B. is supported by grant R01-GM58553 from the NIH (U.S.A.). M.D.H. is supported by the U.K. Medical Research Council (G8604010), the European Union (QLK-CT-2002-02149) and the Wellcome Trust for capital equipment (Confocal; Improvision). M. D. H. and G. B. B. thank the Wellcome Trust for a Research Collaborative (Travel) Grant. DNA sequencing and oligonucleotide synthesis were supported by award 5-PO-CA42014 from the NCI, NIH.

REFERENCES

1 Conti, M. (2000) Phosphodiesterases and cyclic nucleotide signaling in endocrine cells. Mol. Endocrinol. **14**, 1317–1327
2 Houslay, M. D. (2001) PDE4 cAMP-specific phosphodiesterases. Prog. Nucleic Acid Res. Mol. Biol. **69**, 249–315
3 Houslay, M. D., Sullivan, M. and Bolger, G. B. (1998) The multienzyme PDE4 cyclic AMP-specific phosphodiesterase family: Intracellular targeting, regulation, and selective inhibition by compounds exerting anti-inflammatory and anti-depressant actions. Adv. Pharmacol. **44**, 225–342
4 Beavo, J. A. (1995) Cyclic nucleotide phosphodiesterases: functional implications of multiple isoforms. Physiol. Rev. **75**, 725–748
5 Bolger, G., Michaeli, T., Martins, T., St. John, T., Steiner, B., Rodgers, L., Riggs, M., Wigler, M. and Ferguson, K. (1993) A family of human phosphodiesterases homologous to the *dunce* learning and memory gene product of *Drosophila melanogaster* are potential targets for antidepressant drugs. Mol. Cell. Biol. **13**, 6558–6571
6 Bolger, G. B., Erdogan, S., Jones, R. E., Loughney, K., Wilkinson, I., Scotland, G., Hoffman, R., Farrell, C. and Houslay, M. D. (1997) Characterization of five different proteins produced by alternatively spliced mRNAs from the human cAMP-specific phosphodiesterase PDE4D gene. Biochem. J. **328**, 539–548
7 Bolger, G. B., McPhee, I. and Houslay, M. D. (1996) Alternative splicing of cAMP-specific phosphodiesterase mRNA transcripts. Characterization of a novel tissue-specific isoform, RNPDE4A8. J. Biol. Chem. **271**, 1065–1071
8 Huston, E., Lumb, S., Russell, A., Catterall, C., Ross, A., Steele, M. R., Bolger, G. B., Perry, M. J., Owens, R. J. and Houslay, M. D. (1997) Molecular cloning and transient expression in COS cells of a novel human PDE4B cyclic AMP-specific phosphodiesterase, HSPDE4B3. Biochem. J. **328**, 549–556
9 Sette, C., Vicini, E. and Conti, M. (1994) The ratPDE3/IVd phosphodiesterase gene codes for multiple proteins differentially activated by cAMP-dependent protein kinase. J. Biol. Chem. **269**, 18271–18274
9a Erratum (1994) J. Biol. Chem. **269**, 20806
10 Bolger, G. B., Rodgers, L. and Riggs, M. (1994) Differential CNS expression of alternative mRNA isoforms of the mammalian genes encoding cAMP-specific phosphodiesterases. Gene **149**, 237–244

11 Iona, S., Cuomo, M., Bushnik, T., Naro, F., Sette, C., Hess, M., Shelton, E. R. and Conti, M. (1998) Characterization of the rolipram-sensitive, cyclic AMP-specific phosphodiesterases: identification and differential expression of immunologically distinct forms in the rat brain. Mol. Pharmacol. **53**, 23–32

12 McPhee, I., Cochran, S. and Houslay, M. D. (2001) The novel long PDE4A10 cyclic AMP phosphodiesterase shows a pattern of expression within brain that is distinct from the long PDE4A5 and short PDE4A1 isoforms. Cell. Signalling **13**, 911–918

13 Morena, A. R., Boitani, C., de Grossi, S., Stefanini, M. and Conti, M. (1995) Stage and cell-specific expression of the adenosine 3′,5′ monophosphate-phosphodiesterase genes in the rat seminiferous epithelium. Endocrinology **136**, 687–695

14 Beard, M. B., Olsen, A. E., Jones, R. E., Erdogan, S., Houslay, M. D. and Bolger, G. B. (2000) UCR1 and UCR2 domains unique to the cAMP-specific phosphodiesterase family form a discrete module via electrostatic interactions. J. Biol. Chem. **275**, 10349–10358

15 Hoffmann, R., Wilkinson, I. R., McCallum, J. F., Engels, P. and Houslay, M. D. (1998) cAMP-specific phosphodiesterase HSPDE4D3 mutants which mimic activation and changes in rolipram inhibition triggered by protein kinase A phosphorylation of Ser-54: generation of a molecular model. Biochem. J. **333**, 139–149

16 Lim, J., Pahlke, G. and Conti, M. (1999) Activation of the cAMP-specific phosphodiesterase PDE4D3 by phosphorylation. Identification and function of an inhibitory domain. J. Biol. Chem. **274**, 19677–19685

17 MacKenzie, S. J., Baillie, G. S., McPhee, I., Bolger, G. B. and Houslay, M. D. (2000) ERK2 mitogen-activated protein kinase binding, phosphorylation, and regulation of the PDE4D cAMP-specific phosphodiesterases. The involvement of COOH-terminal docking sites and NH2-terminal UCR regions. J. Biol. Chem. **275**, 16609–16617

18 Sette, C. and Conti, M. (1996) Phosphorylation and activation of a cAMP-specific phosphodiesterase by the cAMP-dependent protein kinase. Involvement of serine 54 in the enzyme activation. J. Biol. Chem. **271**, 16526–16534

19 Sette, C., Iona, S. and Conti, M. (1994) The short-term activation of a rolipram-sensitive, cAMP-specific phosphodiesterase by thyroid-stimulating hormone in thyroid FRTL-5 cells is mediated by a cAMP-dependent phosphorylation. J. Biol. Chem. **269**, 9245–9252

20 McLaughlin, M. M., Cieslinski, L. B., Burman, M., Torphy, T. J. and Livi, G. P. (1993) A low-K_m, rolipram-sensitive, cAMP-specific phosphodiesterase from human brain. Cloning and expression of cDNA, biochemical characterization of recombinant protein, and tissue distribution of mRNA. J. Biol. Chem. **268**, 6470–6476

21 Obernolte, R., Bhakta, S., Alvarez, R., Bach, C., Zuppan, P., Mulkins, M., Jarnagin, K. and Shelton, E. R. (1993) The cDNA of a human lymphocyte cyclic-AMP phosphodiesterase (PDE IV) reveals a multigene family. Gene **129**, 239–247

22 Swinnen, J. V., Tsikalas, K. E. and Conti, M. (1991) Properties and hormonal regulation of two structurally related cAMP phosphodiesterases from the rat Sertoli cell. J. Biol. Chem. **266**, 18370–18377

23 Jin, S. L. and Conti, M. (2002) Induction of the cyclic nucleotide phosphodiesterase PDE4B is essential for LPS-activated TNF-alpha responses. Proc. Natl. Acad. Sci. U.S.A. **99**, 7628–7633

24 Barnes, P. J. (2000) Chronic obstructive pulmonary disease. N. Engl. J. Med. **343**, 269–280

25 Giembycz, M. A. (2000) Phosphodiesterase 4 inhibitors and the treatment of asthma: where are we now and where do we go from here? Drugs **59**, 193–212

26 Schudt, C., Tenor, H. and Hatzelmann, A. (1995) PDE isoenzymes as targets for anti-asthma drugs. Eur. Respir. J. **8**, 1179–1183

27 Souness, J. E. and Rao, S. (1997) Proposal for pharmacologically distinct conformers of PDE4 cyclic AMP phosphodiesterases. Cell. Signalling **9**, 227–236

28 Timmer, W., Leclerc, V., Birraux, G., Neuhauser, M., Hatzelmann, A., Bethke, T. and Wurst, W. (2002) The new phosphodiesterase 4 inhibitor roflumilast is efficacious in exercise-induced asthma and leads to suppression of LPS-stimulated TNF-alpha ex vivo. J. Clin. Pharmacol. **42**, 297–303

29 Torphy, T. J. (1998) Phosphodiesterase isozymes: molecular targets for novel antiasthma agents. Am. J. Respir. Crit. Care Med. **157**, 351–370

30 Huston, E., Beard, M., McCallum, F., Pyne, N. J., Vandenabeele, P., Scotland, G. and Houslay, M. D. (2000) The cAMP-specific phosphodiesterase PDE4A5 is cleaved downstream of its SH3 interaction domain by caspase-3. Consequences for altered intracellular distribution. J. Biol. Chem. **275**, 28063–28074

31 McPhee, I., Pooley, L., Lobban, M., Bolger, G. and Houslay, M. D. (1995) Identification, characterization and regional distribution in brain of RPDE-6 (RNPDE4A5), a novel splice variant of the PDE4A cyclic AMP phosphodiesterase family. Biochem. J. **310**, 965–974

32 Shakur, Y., Wilson, M., Pooley, L., Lobban, M., Griffiths, S. L., Campbell, A. M., Beattie, J., Daly, C. and Houslay, M. D. (1995) Identification and characterization of the type-IVA cyclic AMP-specific phosphodiesterase RD1 as a membrane-bound protein expressed in cerebellum. Biochem. J. **306**, 801–809

33 Sambrook, J. and Russell, D. W. (2001) Molecular Cloning: A Laboratory Manual, 3rd edn, Cold Spring Harbor Laboratory Press, Cold Spring Harbor, NY

34 Colicelli, J., Birchmeier, C., Michaeli, T., O'Neill, K., Riggs, M. and Wigler, M. (1989) Isolation and characterization of a mammalian gene encoding a high-affinity cAMP phosphodiesterase. Proc. Natl. Acad. Sci. U.S.A. **86**, 3599–3603

35 Kozak, M. (1989) The scanning model for translation: an update. J. Cell Biol. **108**, 229–241

36 Hopp, T. P., Prickett, K. S., Price, V. L., Libby, R. T., March, C. J., Cerretti, D. P., Urdal, D. L. and Conlon, P. J. (1988) A short polypeptide marker sequence useful for recombinant protein identification and purification. Biotechnology **6**, 1204–1210

37 Baillie, G., MacKenzie, S. J. and Houslay, M. D. (2001) Phorbol 12-myristate 13-acetate triggers the protein kinase A-mediated phosphorylation and activation of the PDE4D5 cAMP phosphodiesterase in human aortic smooth muscle cells through a route involving extracellular signal regulated kinase (ERK). Mol. Pharmacol. **60**, 1100–1111

38 MacKenzie, S. J. and Houslay, M. D. (2000) Action of rolipram on specific PDE4 cAMP phosphodiesterase isoforms and on the phosphorylation of cAMP-response-element-binding protein (CREB) and p38 mitogen-activated protein (MAP) kinase in U937 monocytic cells. Biochem. J. **347**, 571–578

39 Harlow, E. and Lane, D. P. (1990) Antibodies: A Laboratory Manual, Cold Spring Harbor Laboratory Press, Cold Spring Harbor, NY

40 Marchmont, R. J. and Houslay, M. D. (1980) A peripheral and an intrinsic enzyme constitute the cyclic AMP phosphodiesterase activity of rat liver plasma membranes. Biochem. J. **187**, 381–392

41 Bradford, M. M. (1976) A rapid and sensitive method for the quantitation of microgram quantities of protein utilizing the principle of protein-dye binding. Anal. Biochem. **72**, 248–254

42 Milatovich, A., Bolger, G., Michaeli, T. and Francke, U. (1994) Chromosome localizations of genes for five cAMP-specific phosphodiesterases in man and mouse. Somat. Cell Mol. Genet. **20**, 75–86

43 Loughney, K. and Ferguson, K. (1996) Identification and quantification of PDE isoenzymes and subtypes by molecular biological methods. In The Handbook of Immunopharmacology: Phosphodiesterase Inhibitors (Schudt, C., Dent, G. and Rabe, K. F., eds.), pp. 1–19, Academic Press, San Diego

44 MacKenzie, S. J., Baillie, G. S., McPhee, I., MacKenzie, C., Seamons, R., McSorley, T., Millen, J., Beard, M. B., Van Heeke, G. and Houslay, M. D. (2002) Long PDE4 cAMP specific phosphodiesterases are activated by protein kinase A-mediated phosphorylation of a single serine residue in Upstream Conserved Region 1 (UCR1). Br. J. Pharmacol. **136**, 421–433

45 Tobias, E. S., Rozengurt, E., Connell, J. M. and Houslay, M. D. (1997) Co-transfection with protein kinase D confers phorbol-ester-mediated inhibition on glucagon-stimulated cAMP accumulation in COS cells transfected to overexpress glucagon receptors. Biochem. J. **326**, 545–551

46 Qiu, Y. H., Chen, C. N., Malone, T., Richter, L., Beckendorf, S. K. and Davis, R. L. (1991) Characterization of the memory gene *dunce* of *Drosophila melanogaster*. J. Mol. Biol. **222**, 553–565

47 Sullivan, M., Rena, G., Begg, F., Gordon, L., Olsen, A. S. and Houslay, M. D. (1998) Identification and characterization of the human homologue of the short PDE4A cAMP-specific phosphodiesterase RD1 (PDE4A1) by analysis of the human HSPDE4A gene locus located at chromosome 19p13.2. Biochem. J. **333**, 693–703

48 Olsen, A. E. and Bolger, G. B. (2000) Physical mapping and promoter structure of the murine cAMP-specific phosphodiesterase pde4a gene. Mamm. Genome **11**, 41–45

49 Dodge, K. L., Khouangsathiene, S., Kapiloff, M. S., Mouton, R., Hill, E. V., Houslay, M. D., Langeberg, L. K. and Scott, J. D. (2001) mAKAP assembles a protein kinase A/PDE4 phosphodiesterase cAMP signaling module. EMBO J. **20**, 1921–1930

50 Jin, S. C., Bushnik, T., Lan, L. and Conti, M. (1998) Subcellular localization of rolipram-sensitive, cAMP-specific phosphodiesterases. Differential targeting and activation of the splicing variants derived from the pde4d gene. J. Biol. Chem. **273**, 19672–19678

51 Tasken, K. A., Collas, P., Kemmner, W. A., Witczak, O., Conti, M. and Tasken, K. (2001) Phosphodiesterase 4D and protein kinase a type II constitute a signaling unit in the centrosomal area. J. Biol. Chem. **276**, 21999–22002

52 Yarwood, S. J., Steele, M. R., Scotland, G., Houslay, M. D. and Bolger, G. B. (1999) The RACK1 signaling scaffold protein RACK1 selectively interacts with the cAMP-specific phosphodiesterase PDE4D5 isoform. J. Biol. Chem. **274**, 14909–14917

Received 10 July 2002/19 November 2002; accepted 20 November 2002
Published as BJ Immediate Publication 20 November 2002, DOI 10.1042/BJ20021082